

Application of graphene oxide as (nano) reinforcement in epoxy composites

Aplicação de óxido de grafeno como (nano) reforço em compósito de matriz epóxi

Elilton Rodrigues Edwards¹, Érica Cristina Almeida¹,
Marivaldo Batista dos Santos¹, Alan Santos Oliveira¹

¹Department of Exact Science and Technology, State University of Santa Cruz - UESC, Rodovia Jorge Amado, Km 16, Salobrinho CEP: 45.662-900, Ilhéus, BA, Brazil.
e-mail: eredwards@uesc.br, ecalmeida@uesc.br, marivaldobsj@gmail.com, alansoraths@gmail.com

ABSTRACT

Composite with nanometric particles have been used as a structural reinforcement to improve the mechanical properties in polymeric materials. The use of graphene has shown excellent results such as Young's modulus of 1 TPa, tensile strength of about 130 GPa, thermal conductivity of 5000 W/mK, electrical conductivity of up to 6000 S/cm, in addition to presenting great carrier mobility of loads of $2 \times 10^5 \text{ cm}^2 \cdot \text{V}^{-1} \cdot \text{s}^{-1}$. Thus, the mechanical properties in the epoxy resin based on diglycidyl ether of bisphenol A were evaluated with the addition of increasing percentages of graphene oxide (GO) in order to evaluate the mechanical properties in this material. The synthesis of GO was made from natural graphite by the Hummers method. The nanostructured composites were manufactured with a mixture of 0.1%, 0.2%, 0.5% and 1% by weight of GO. The characterizations of the materials were made by FTIR-ATR, DRX, RAMAN, MEV and TGA. The mechanical properties were evaluated by increasing the impact energy Izod absorbed in composites with lower GO content. The results showed that with the increase in the amount of graphene oxide there was an increase in the mechanical properties and that the increase in the OG charge in the matrix generated agglomerations, impairing the impact absorption in the mechanical properties of the material making it necessary a rigorous process of dispersion of these nanometric materials in the polymeric matrix.

Keywords: Graphene oxide synthesis, mechanical properties, nanostructured composite.

RESUMO

Compósito com partículas nanométricas tem sido utilizado como reforço estrutural para melhoria das propriedades mecânicas em materiais poliméricos. A utilização de grafeno tem apresentado excelentes resultados tais como módulo de Young de 1 TPa, resistência à tração de cerca de 130 GPa, condutividade térmica de 5000 W/mK, condutividade elétrica de até 6000 S/cm, além de apresentar grande mobilidade de portadores de cargas de $2 \times 10^5 \text{ cm}^2 \cdot \text{V}^{-1} \cdot \text{s}^{-1}$. Dessa forma, foram avaliadas as propriedades mecânicas na resina epóxi à base de éter diglicidílico do bisfenol A com adição de porcentagens crescentes de óxido de grafeno (GO) a fim de avaliarmos as propriedades mecânicas neste material. A síntese do GO foi feita a partir da grafite natural pelo método de Hummers. Os compósitos nanoestruturados foram fabricados com uma mistura de 0.1%, 0.2%, 0.5% e 1% em peso de GO. As caracterizações dos materiais foram feitas por análises de FTIR-ATR, DRX, RAMAN, MEV e TGA. As propriedades mecânicas foram avaliadas pelo aumento da energia de impacto Izod absorvida em compósitos com menor teor de GO. Os resultados mostraram que com o aumento da quantidade de óxido de grafeno houve um aumento nas propriedades mecânicas e que o aumento da carga de OG na matriz gerou aglomerações prejudicando a absorção do impacto nas propriedades mecânicas do material, tornando necessário um rigoroso processo de dispersão desses materiais nanométrico na matriz polimérica.

Palavras-chave: Síntese de óxido de grafeno, propriedades mecânicas, compósitos nanoestruturados.

1. INTRODUÇÃO

Graphene-based nanocomposites have been of great importance in the development of research in new materials due to their excellent properties such as Young modulus of 1 TPa, tensile strength of about 130 GPa,

thermal conductivity of 5000 W/(mK) and electrical conductivity of up to 6000 S/cm [1, 2]. One of the main applications of graphene occurs in structural reinforcement in the manufacture of polymeric nanocomposites, thus allowing a better utilization of the properties of both materials such as the easy processability of the polymers added to the hardness and resistance of the graphene [3]. Graphene oxide (GO), despite having lower properties than graphene, is easy to manufacture in large quantities with exceptional properties, high flexibility and high bonding potential, which allows its application in various areas such as biosensors, storage energy, electronics and especially in polymer composites [4, 5].

The use of these materials in composite fabrication enables the increase in the properties of reinforced materials such as shear modulus, toughness, optical properties, electrical conductivity and many others with only small amounts of dispersed graphene oxide particles in the polymer matrix [6]. Thus, graphene oxide has been used to manufacture reinforced nanostructured epoxy matrix composites and, subsequently, improve the mechanical properties of these composites. However, one of the major problems in the mixing process of these materials is the formation of agglomerates that may be detrimental to the final mechanical properties of the composites. Thus, solvents such as water, ethanol, tetrahydrofuran and acetone are used to enable a more homogeneous dispersion between matrix and reinforcement in the polymer composite [7].

Several studies show that the mechanical properties of composite materials increase with the addition of graphene oxide [8-11]. This oxide acts as a structural reinforcement enabling an increase in the Young's module of the material. And this characteristic has led to a wide study of this material as a structural reinforcement in engineering

The present study evaluated the mechanical properties of diglycidyl ether of bisphenol A (DGEBA) epoxy resin composites with increasing percentages of graphene oxide synthesized from natural graphite by the modified Hummers method. The obtained GO was characterized by infrared spectroscopy, X-ray diffraction, Raman spectroscopy, scanning electron microscopy and thermogravimetry. Moreover, the composites were characterized by infrared spectroscopy and scanning electron microscopy to analyze the degree of cure and dispersion of these materials. The mechanical behaviors of the composites obtained were further evaluated by the Izod impact test.

2. MATERIALS AND METHODS

2.1 Graphene oxida synthesis

Graphene oxide (GO) synthesis was performed based on Hummers and Offeman method [12], using graphite as a starting material. For the reaction 8 g of graphite, 4 g of sodium nitrate (NaNO_3) and 184 mL of concentrated sulfuric acid (H_2SO_4) were mixed with magnetic stirring in an ice bath. After 15 minutes, 320 mL of water at about 60°C and 26.16 mL of hydrogen peroxide (H_2O_2) were added to reduction the residual permanganate and of the bubbles generated. Finally, the system was placed in an Erlenmeyer where was diluted with water to pH 7. After this stage, part of the material was dried in an oven at 120 °C for 2 hours (for use of graphite oxide) and the rest was sonicated in an ultrasound bath for 15 minutes (for use of graphene oxide) which was then oven dried at 120°C for 2 hours.

2.2 Nanocomposites fabrication

The nano composites were produced using diglycidyl ether of bisphenol A (DGEBA) epoxy resin and cycloaliphatic amine-based hardener at a 2:1 mass ratio (resin/hardener) and 0.1%, 0.2%, 0.5% and 1% of GO were used in relation to the weight of the resin. The GOs were dispersed in acetone with magnetic stirring for 5 minutes. Subsequently, the mixture was added to the resin with magnetic stirring and heating at 70°C for 30 minutes to decrease viscosity and facilitate dispersion of carbonaceous material and evaporation of acetone. The material underwent a degassing process using a vacuum pump to eliminate air bubbles and solvent misconceptions. The hardener was added to the mixture with magnetic stirring and placed in silicone molds for curing at room temperature for 24 h followed by post curing in an oven at 80°C for 4 hours.

2.3 Characterization

Graphene oxide was characterized by scanning electron microscopy (SEM) with a Quanta 250 microscope, with vCD detector, working distance (WD) of 7 mm, energy of 15 kV and spot probe 4.0 for topographic evaluation and characterization of the graphene layers. The composites were metalized with gold for their characterization by SEM. Structural characterizations of graphene oxide were made by X-ray analysis with a Rigaku miniflex 600 diffractometer, using a Cu $K\alpha$ radiation, 2θ ranging from 5 to 80° with a scanning speed

of 20°/min at 40 Kv and 15. FTIR analysis was performed on an i510 SMART OMNI-Transmission spectrophotometer with a spectral range of 4000 to 400 cm^{-1} in ATR (Attenuated Total Reflectance) mode for identification of functional groups in the GO and analysis of the open-curing process of the epoxy ring of composites. Raman spectroscopy was performed using a Renishaw 2000 system equipped with an Air laser (514.5 nm), ranging from 1000 to 3500 cm^{-1} , to verify the integrity of the graphene powder after each treatment, based on the relative band intensity D and G, (ID/IG) [13, 14]. The mechanical properties of the nanostructured composite were evaluated by Izod impact test on a Panantec ATMI impact pendulum, model PID-22, following ASTM D256, using 11 J impact hammer at 3.5 m descending speed/s and impact resistance measurement unit in kJ m. Graphite and GO mass loss analysis was performed using Shimadzu model DTG 60 equipment in a dynamic nitrogen atmosphere at a speed of 10°C min^{-1} from 0°C to 800°C.

The thermogravimetric analysis (TGA) of graphene oxide mass loss was done using a Shimadzu equipment, model DTG 60 in atmosphere of nitrogen with velocity of 10°C min^{-1} , with start of 0°C to 800°C, in an open aluminum crucible. The analyzed samples had a mass of about 5 mg in powder. The analyzes were based on the international standard ASTM E 1641/16, which addresses kinetic decomposition in thermogravimetric analysis based on the main known methods (Ozawa / Flynn / Wall Method) for this thermal characterization. The GO curve presented 4 characteristic regions of mass loss: the first region from approximately 19°C to 100°C; a second mass loss from 100°C to 250°C; a third mass loss between 250°C and 500°C; and the final mass loss above 500°C. According to Chiu et al. [22], mass loss before 100°C was attributed to the desorption of water molecules. Second region of mass loss was associated with the release of carbon dioxide (CO_2), carbon monoxide (CO) and water (H_2O) [23].

3. RESULTS AND DISCUSSION

3.1 Graphene oxide characterization

Figure 1 shows SEM images of the morphology of pure graphite and graphene oxide with several overlapping sheets mostly in hexagonal shape. Figure-1a and 1b refer to graphite and Figure 1c and 1d refer to graphene oxide (GO). From Figure 1c, a separation between the graphite layers was observed due to factors such as sonication, which creates separation between the sheets, and also the high oxygen content between the graphene sheets [7, 15].

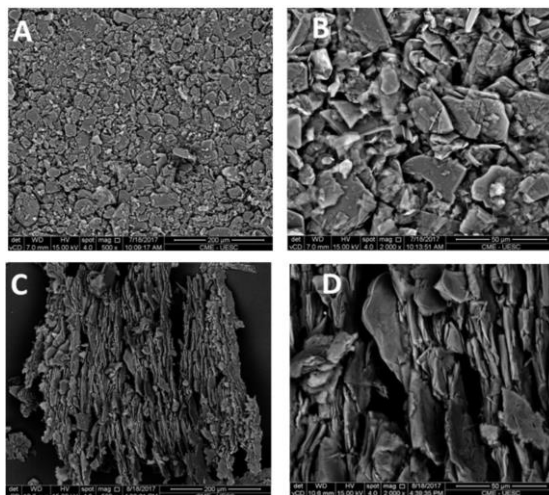


Figure 1: SEM of (a) graphite structure, (b) 4x increase and (c) graphene oxide, (d) 4x increase.

Figure 2 shows the infrared spectra normalized of (a) graphite and (b) graphene oxide (GO) and indicates the presence of oxygenated groups such as hydroxyl (O-H) at 3208 cm^{-1} [16], carbonyl (C=O) at 1714 cm^{-1} , carbon double bond (C=C) at 1621 cm^{-1} [17] and epoxy (CO) at 1372 cm^{-1} [18] in structure from GO. The presence of these functional groups in the graphite structure is indicative of the oxidation process.

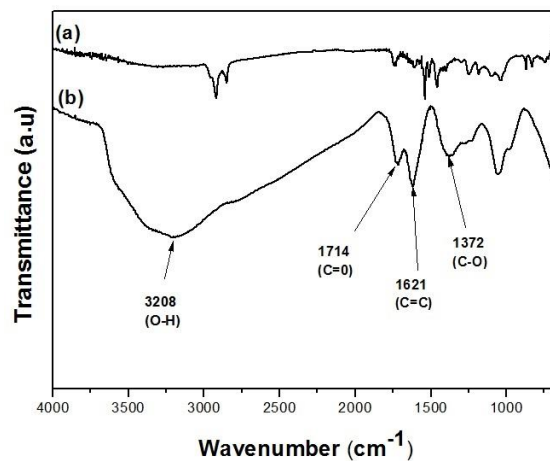


Figure 2: FTIR-ATR analysis on (a) graphite and (b) graphene oxide.

Figure 3 shows the XRD spectrum normalized of graphite and GO and reveals two incident peaks for the graphite spectrum in the 26° region relative to plane (002) [19] and a lower intensity peak in the region 54° concerning the plane (004) [20]. The broadening of the GO spectrum shows a lower intensity peak in the 26° region and the appearance of a peak in the 11° region relative to the plane (001) [21]. This peak is characteristic of the oxidation process due to the insertion of functional groups in which the higher the intensity the higher the oxidation level of the material.

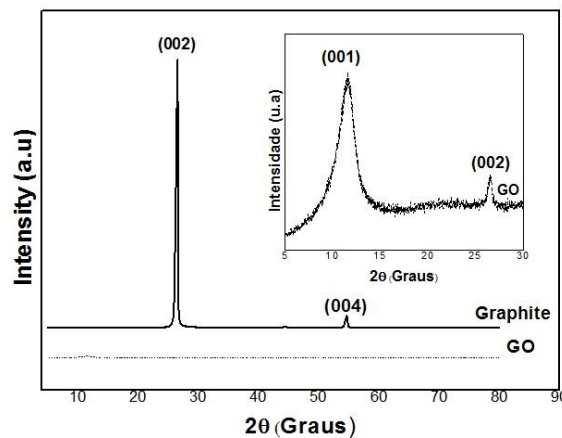


Figure 3: Graphite and GO DRX diffraction spectrum.

Figure 4 shows the graph of thermogravimetry analysis (TGA) with the information on the loss of mass of graphene and graphene oxide with increasing temperature. These analyzes were made in order to understand the thermal stability and the consequences of the different degrees of oxygen functionalization in the GO samples synthesized for use in the manufacture of the composite. The analysis was carried out with nitrogen flow at a rate of 50 mL/min and a heating rate of 10°C/min starting at 0°C to 800°C. Graphite remained stable with increasing temperature. The loss of mass occurs at around 100°C, mainly due to the loss of H₂O molecules interspersed between the layers of the GO sheet [33]. The graphite oxide (GO) showed a decrease in thermal stability at a temperature of about 200°C due to the decomposition of carboxylates and the release of CO₂ [32]. The third region, starting at 500°C, showed a greater loss of mass that was attributed to the removal of oxygenated groups such as hydroxyl, carbonyl and epoxy [24]. Above 600°C, this loss was attributed to the rapid combustion of carbon, being an indication of the thermal stability of the carbon structure in the oxide samples [14, 33].

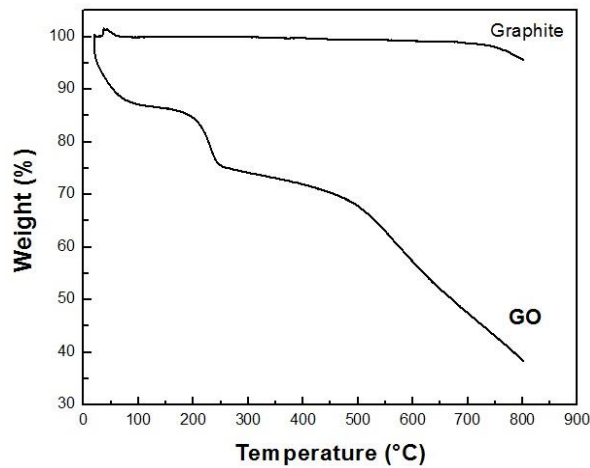


Figure 4: Graphite and GO thermogravimetric analysis curves (TGA)

Figure 5 shows the Raman spectrum of graphite with the presence of bands D and G at positions 1327 cm^{-1} and 1580 cm^{-1} , respectively and band G' at 2682 cm^{-1} . The GO oxide spectrum, in addition to bands D and G corresponding to positions 1329 cm^{-1} and 1571 cm^{-1} , indicates the 2D band (or G') at 2662 cm^{-1} , where the GO spectrum shifts relative to graphite. It was possible to calculate the ratio between the bands identified in graphite (Table 1). The graphite band (G) has a much higher intensity than the disorder band (D), which characterizes a material with a high degree of crystallinity. GO presented a higher intensity D band in relation to the G band, compared to the graphite band, observed by the increase of the I_D/I_G index ratio, thus characterizing a more disordered material resulting from the oxidation and exfoliation process that generates defects in the crystalline structure of graphite due to the addition of oxygenated groups to its structure [13]. Through the value of the ratio I_{2D}/I_G , it was verified that for the value found for the GO, there is the formation of multiple layers of graphene sheets, since the value presented is less than 1 [14].

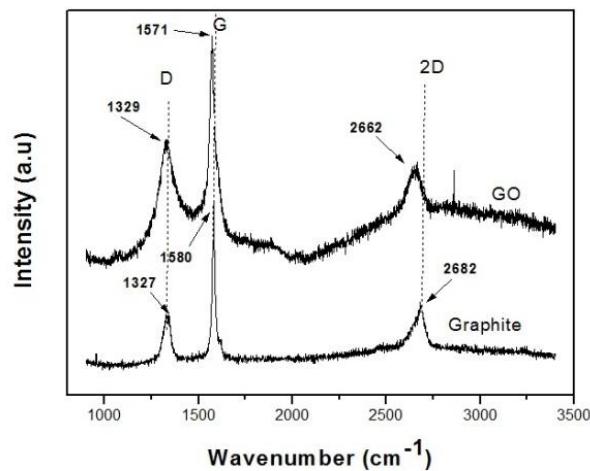


Figura 5: Graphite and GO Raman spectra.

Table 1: Relation of D, G, 2D peak intensities and I_D/I_G and I_{2D}/I_G ratio for graphite and GO samples.

SAMPLE	BANDS D (a.u)	BANDS G (a.u)	BANDS 2D (a.u)	I_D/I_G	I_{2D}/I_G
Graphite	466	1106	534	0.42	0.48
GO	1458	2056	1338	0.71	0.65

3.1 Nanocomposites characterization

Figure 6 shows the topographic SEM image of the surface of specimens containing pure resin and resin containing percentages of GO after fracture by Izod impact test. Figure 6a, without the addition of GO reinforcement, shows a smoother surface indicating a fragile fracture. Figures 6b, 6c and 6d reveal the morphology of a rougher fracture characteristic of a more ductile material. Thus, when large amounts of GO are added, the amount of lamellar structure decreases, which is characterized by fragile material. On the other hand, when a small amount of GO is added, a large amount of lamellar structure is formed, which is characterized by ductile material. These results indicate that the formation of a new composite layer occurred with the addition of GO [24-29].

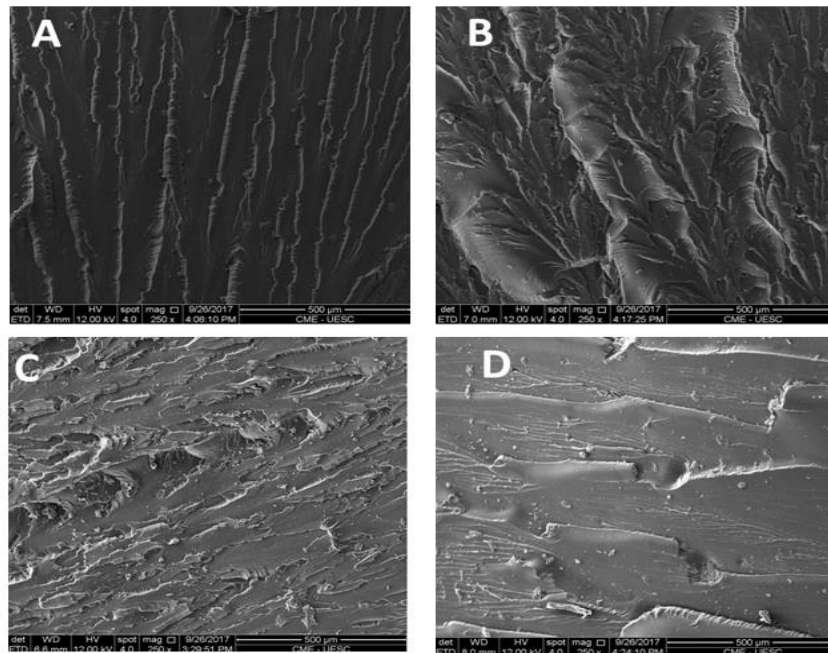


Figure 6: SEM image of composite topography with (a) pure resin and resin containing different percentages of GO (b) 0.1%, (c) 0.2% and (d) 0.5%.

Figure 7 shows the fractured composite containing 1% GO with a rougher agglomerate surface as indicated by the arrow in the enlarged region. The formation of these agglomerates caused the composite to have a lower impact absorption energy.

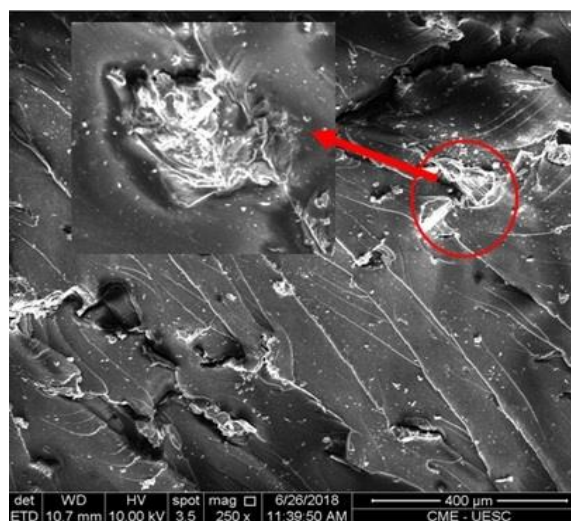


Figure 7: SEM image of composite topography with 1% GO indicating fractured surface.

Figure 8 shows the infrared spectra of pure resins and diglycidyl ether of bisphenol A catalyst-cured resin. This figure shows that the region between 1180 cm^{-1} and 1610 cm^{-1} corresponds to the region of interaction between the epoxy group and the hardener amine with the ring opening [25]. The 830 cm^{-1} region can be associated with symmetrical deformations of the C-O-C bonding plane [26]. The presence of characteristic bands in the region of 1250 cm^{-1} corresponds to the symmetrical axial deformation of the epoxy ring. This region contains epoxy rings indicating the degree of cure of the resin. The smaller the number of rings in that region the greater the degree of cure [7]. Thus, it was observed that the resin was completely cured at the submitted temperature of $80^{\circ}\text{C}/4\text{h}$.

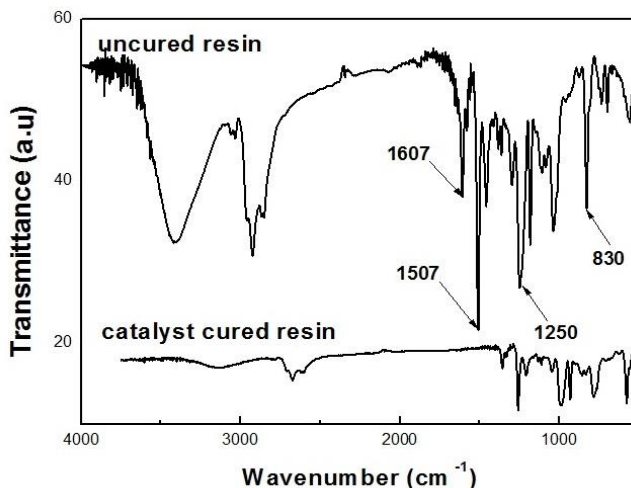


Figure 8: FTIR/ATR results with identified peaks of (a) pure resins and (b) cured with diglycidyl ether of bisphenol A based catalyst.

Figure 9 shows the FTIR spectrum of the resin without GO compared to the composite with 0.1, 0.2, 0.5 and 1.0% GO. A comparison of the pure composite with the composite containing different percentages of GO reveals that the 787 cm^{-1} band changed to an 828 cm^{-1} domain related to the reaction progress (see $2000\text{-}300\text{ cm}^{-1}$ region in the graph).

Thus, the presence of GO increased the degree of polymerization of these samples. The 1050 cm^{-1} bands are assigned the band (C-C-C) that is associated with the presence of the GO. The 1250 cm^{-1} band is attributed to the vibrations of groups (C-O-C) belonging to the synthesis of GO. The emergence and increase of the 1508 cm^{-1} band can be attributed to the increased bond (C=C) during the curing process of the epoxy resin. The emergence of the 2362 cm^{-1} band is attributed to the bond (C≡C), probable contamination, that disappears with increasing percentages of GO. The band at 2930 cm^{-1} is attributed to the primary and secondary carbons (CH_3 , CH_2) and increases as the percentage of GO in the composite increases [27].

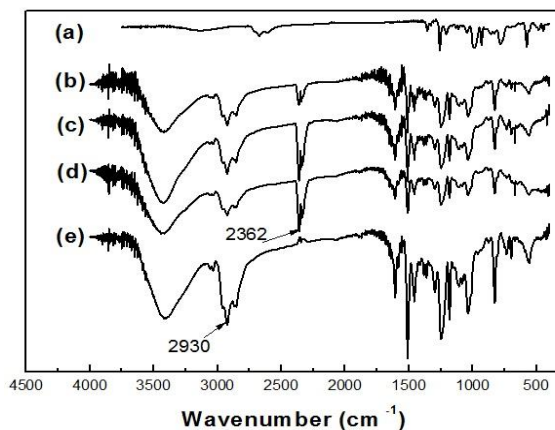


Figure 9: FTIR/ATR with identified peaks of (a) resins without GO, (b) 0.1% GO cured resins, (c) 0.2%, (d) 0.5% and (e) 1.0%.

Figure 10 and Table 2 show the results of the Izod impact test on specimens, where composites with GO weight gain by 0.1% and 0.2% increased by 34.5% and 266.5% in relation to resistance to the impact of pure resin. However, a large variation was observed in standard deviation and some values of specimens containing 0.1% of GO had a lower energy absorption value compared to the standard. This may have been a result of the difficulty of GO homogenization in the specimen, causing a variation among the tested materials. The composites containing 0.5% of GO had the highest impact absorption rate, with an increase of 274.6% in relation to the reference, due to a larger load dispersion without the formation of agglomerates.

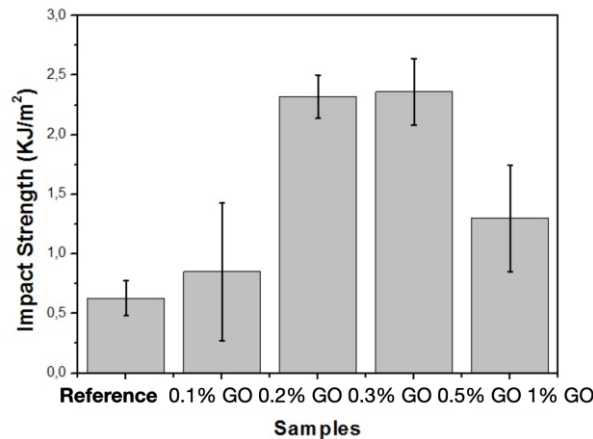


Figure 10: Graph of the energy absorbed by the test specimens in the impact test.

The composites containing 1% of GO increased by 177.7% in relation to the reference but the value of the absorbed energy decreased compared to the composite with 0.5% and 0.2%. This decrease of absorbed energy may have been due to the formation of agglomerates that resulted in low interfacial adhesion between resin and reinforcement. According to Kang [28], the increased strength in GO-reinforced composites is due to the strong hydrogen bond between the GO and resin functional groups. High concentrations of functional groups can lead to a decrease in the mechanical properties of materials, such as the Young's module [30]. The mechanical properties of composite materials with GO are related to the increase in the amount of GO up to a limit of 1.0%. The addition of values above 1.0% causes the formation of agglomerates that decrease the mechanical properties of the material instead of increasing it. A similar problem has also been observed with the addition of functionalized carbon nanotubes in resin [25]. Another factor to be observed is that with the increase of the functional groups above a determined limit value, there will be a breakdown of important chemical bonds decreasing the mechanical properties of the material. In this case, a decrease in mechanical properties is observed instead of increasing. Similar observations were also made in [31]. Thus, the composite with Resin + 1.0% GO showed a decrease in absorption energy.

Table 2: Energy absorbed values at post-cure temperatures of 80°C and their standard deviations.

COMPOSITES	ABSORBED ENERGY (10 KJ/m ² , 80°C)
Resin	0.63±0.15
Resin + 0.1% GO	0.85±0.58
Resin + 0.2% GO	2.23±0.18
Resin + 0.5% GO	2.36±0.28
Resin + 1.0% GO	1.30±0.45

4. CONCLUSION

In this study we observed the influence of the addition of graphene oxide in different percentages (0.1%, 0.2%, 0.5% and 1%) in an epoxy matrix and evaluated resistance to Izod impact. Impact resistance tended to increase for composites from 0.1% to 0.5% with GO and showed the best result with a 254% increase compared to the benchmark composite. Impact resistance decreased for 1% GO composite, due to the formation of agglomerates, which generated stress concentration points, making the material more fragile. Therefore, it was possible to conclude that GO dispersion plays a fundamental role in the mechanical properties of composites and that increasing the mixture of this material in epoxy resin may generate agglomerate formation, which impairs the mechanical properties of impact absorption. Thus, the relationship detected in this study between dispersibility and mechanical properties should be observed when producing nanostructured composites in polymeric matrices. When producing nanostructured composites using GO, a rigorous dispersion process should be performed to obtain more efficient mechanical property results.

5. ACKNOWLEDGMENTS

We would like to thank the Higher Education Personnel Improvement Coordination (CAPES) for funding the project and the Graduate Program in Science and Modeling Materials (PROCIMM) at the State University of Santa Cruz (UESC).

6. BIBLIOGRAPHY

- [1] DRZAL, L. T., QIN, Y., HUANG, Z., "Size effect of graphene nanoplatelets on the morphology and mechanical behavior of glass fiber/epoxy composites". *Journal of Materials Science*, v. 7, n. 51, pp. 3337-3348, 2016.
- [2] ZHENG, Q., SHI, L., ZHENG, Q., *et. al.*, "Structure control of ultra-large graphene oxide sheets by the Langmuir-Blodgett method". *RSC Advances*, v. 3, n. 14, pp. 4680-4691, 2013.
- [3] WEI, J., VO, T., INAM, C. C., "Epoxy/graphene nanocomposites processing and properties: a review". *RSC Advances*, v.5, n. 90, pp. 73510-73524, 2015.
- [4] PAPAGEORGIOU, D. G., KINLOCH, I. A., YOUNG, R. J., "Mechanical properties of graphene and graphene-based nanocomposites". *Progress in Materials Science*, v. 90, pp. 75-127, 2017.
- [5] HU, K., KULKARNI, D. D., CHOI, I., *et. al.* "Graphene-polymer nanocomposites for structural and functional applications". *Progress in Polymer Science*, v. 11, n. 39, pp. 1934-1972, 2014.
- [6] JANCAR, J., DOUGLAS, J. F., STARR, F. W., *et. al.*, "Current issues in research on structure-property relationships in polymer nanocomposites". *Polymer*, v. 15, n. 51, pp. 3321-3343, 2010.
- [7] SILVA, D. D., SANTOS, W.D., PEZZIN, S. H., "Nanocompósitos de matriz epoxídica com reforços produzidos a partir do grafite natural". *Revista Matéria*, v. 18, n. 2, pp. 1216-1272, 2013.
- [8] ABDULLAH, S. I., ANSARI, M. N. M. "Mechanical properties of graphene oxide (GO)/epoxy composites". *Hbr Journal*, v. 11, n. 2, p. 151-156, 2015.
- [9] YU, MIN-FENG, *et. al.* "Strength and breaking mechanism of multiwalled carbon nanotubes under tensile load". *Science*, v. 287, n. 5453, p. 637-640, 2000.
- [10] KEYTE, J., PANCHOLI, K., NJUGUNA, J.; "Recent developments in graphene oxide/epoxy carbon fiber-reinforced composites". *Frontiers in materials*, v. 6, p. 224, 2019.
- [11] EQRA, R., MOGHIM, M. H., EQRA, N. "A study on the mechanical properties of graphene oxide/epoxy nanocomposites". *Polymers and Polymer Composites*, p. 09673911211011150, 2021.
- [12] HUMMERS, W. S., OFFEMAN, R. E., "Preparation of graphitic oxide", *Journal of the American Chemical Society*, v. 9, p. 8165-8175, 2015.
- [13] TANG, L. C., WAN, Y. J., YAN, D., *et.al.*, "The effect of graphene dispersion on the mechanical properties of graphene/epoxy composites". *Carbon*, v. 60, pp. 16-27, 2013.
- [14] LAYEK, R. K., NANDI, A. K., "A review on synthesis and properties of polymer functionalized graphene". *Polymer*, v. 54, n. 19, p. 5087-5103, 2013.
- [15] MUZYKA, R., KWOKA, M., *et.al.*, "Oxidation of graphite by different modified Hummers methods". *New Carbon Materials*, v. 1, n. 32, pp. 15-20, 2017.
- [16] OMIDI, S., KAKANEJADIFARD, A., AZARBANI, F. "Noncovalent functionalization of graphene oxide and reduced graphene oxide with Schiff bases as antibacterial agents". *Journal of Molecular Liquids*, v. 242, p. 812-821, 2017.
- [17] DEEMER, E. M., PAUL, P. K., MANCIU, F. S., *et. al.* "Consequence of oxidation method on graphene oxide produced with different size graphite precursors". *Materials Science and Engineering: B*, v. 224, p. 150-157, 2017.

- [18] JIAO, X., ZHANG, L., *et al.*, “Comparison of the adsorption of cationic blue onto graphene oxides prepared from natural graphites with different graphitization degrees”. *Colloids and Surfaces A: Physicochemical and Engineering Aspects*, v. 529, pp. 292-301, 2017.
- [19] LI, Y., CHEN, S., *et al.* “In situ polymerization and mechanical, thermal properties of polyurethane/graphene oxide/epoxy nanocomposites”. *Materials & Design*, v. 47, pp. 850-856, 2013.
- [20] ZHOU, Z., BOUWMAN, W. G., SCHUT, H., *et al.* “Interpretation of X-ray diffraction patterns of (nuclear) graphite”. *Carbon*, v. 69, pp. 17-24, 2014.
- [21] GUPTA, V., SHARMA, N., *et al.* “Higher oxidation level in graphene oxide”. *Optik*, v.143, pp. 115-124, 2017.
- [22] CHIU, P. L., MASTROGIOVANNI, D. D., *et al.* “Microwave-and nitronium ion-enabled rapid and direct production of highly conductive low-oxygen graphene”. *Journal of the American Chemical Society*, v. 13, n. 134, pp. 5850-5856, 2012.
- [23] UHL, F. M., WILKIE, C. A. “Preparation of nanocomposites from styrene and modified graphite oxides”. *Polymer degradation and Stability*, v. 2, n. 84, pp. 215-226, 2004.
- [24] KARIMI, B., RAMEZANZADEH, B., “A comparative study on the effects of ultrathin luminescent graphene oxide quantum dot (GOQD) and graphene oxide (GO) nanosheets on the interfacial interactions and mechanical properties of an epoxy composite”. *Journal of colloid and interface science*, v. 493, p. 62-76, 2017.
- [25] EDWARDS, E. R., KOSTOV, K. G., BOTELHO, E. C., “Evaluation of the chemical interaction between carbon nanotubes functionalized with TGDDM tetrafunctional resin and hardener DDS”. *Composites Part B: Engineering*, v. 51, 197-203, 2013.
- [26] PIRES, G., PEREIRA, D. S., *et al.* “Caracterização físico-química e mecânica do sistema éster de Silsexquioxano/Resina Epóxi Dge-ba/Dietilenotriamina”. *Revista Matéria*, v.2, n. 10, pp. 317-330, 2005.
- [27] EDWARDS, E. R., OISHI, S. S., BOTELHO, E. C. “Analysis of chemical polymerization between functionalized MWCNT and poly (furfuryl alcohol) composite”. *Polímeros*, v. 1, n. 28, pp. 15-22, 2018.
- [28] KANG, W. S., RHEE, K. Y., PARK, S. J., “Thermal, impact and toughness behaviors of expanded graphite/graphite oxide-filled epoxy composites”. *Composites Part B: Engineering*, v. 94, pp. 238-244, 2016.
- [29] YANG, K., *et al.* “The thermo-mechanical response of PP nanocomposites at high graphene loading”. *Nanocomposites*, v. 1, n. 3, p. 126-137, 2015.B
- [30] TAVAKOL, M., *et al.* “Mechanical properties of graphene oxide: The impact of functional groups”. *Applied Surface Science*, v. 525, p. 146554, 2020.
- [31] LIU, L., *et al.* “Mechanical properties of graphene oxides”. *Nanoscale*, v. 4, n. 19, p. 5910-5916, 2012.
- [32] NAJAFI, F., RAJABI, M. “Thermal gravity analysis for the study of stability of graphene oxide–glycine nanocomposites”. *International Nano Letters*, v. 5, n. 4, p. 187-190, 2015.
- [33] DEEMER, E. M., *et al.* “Consequence of oxidation method on graphene oxide produced with different size graphite precursors”. *Materials Science and Engineering: B*, v. 224, p. 150-157, 2017

ORCID

Elilton Rodrigues Edwards	https://orcid.org/0000-0001-5405-8978
Erica Cristina Almeida	https://orcid.org/0000-0002-8390-7315
Marivaldo Batista dos Santos	https://orcid.org/0000-0003-2267-5044
Alan Santos Oliveira	https://orcid.org/0000-0002-3634-5946